KSCE Journal of Civil Engineering (2016) 20(6):2469-2482

DOI 10.1007/s12205-015-0466-1

Structural Engineering

pISSN 1226-7988, eISSN 1976-3808
www.springer.com/12205

Allowable Slope Change of Approach Slabs Based on the Interacted Vibration with Passing Vehicles

Wangchen Yan*, Lu Deng, and Xinfeng Yin*****

Received June 17, 2015/Revised September 1, 2015/Accepted September 29, 2015/Published Online November 13, 2015

Abstract

The slope change of an approach slab can induce a "bumping" effect to passing vehicles, magnify the vehicle impact on the bridge, and accelerate the deterioration of the bridge deck and other components. The allowable slope changes recommended in previous studies, which are usually based on the survey results of ride comfort only, are usually inconsistent. In this study, a three-dimensional vehicle-road-bridge interaction model is developed to study the interaction between passing vehicles and the road and bridge. By fully considering three important aspects, i.e., vehicle's running safety, vehicle users' comfort, and the impact on the bridge, an allowable slope change for approach slab is then proposed based on the recommended limits on the three indexes according to relevant codes. The proposed allowable slope change is considered more rational than previously recommended values and could be used as a reference for engineering practice.

Keywords: *approach slab, slope change, running safety, ride comfort, vehicle impact*

1. Introduction

The primary function of approach slabs is to provide a gradual transition between the bridge deck and the roadway pavement. Slope changes often develop between the bridge abutment and approach slab due to the differential settlement developed between the two ends of the approach slab. A slope change can not only result in a "bumping" effect to passing vehicles and cause rider discomfort but also magnify the impact on the bridge and therefore accelerate the deterioration of the bridge deck and other components, leading to an increase in maintenance expense. In fact, the approach slab is the most important component in bridges for reducing the bump (Briaud *et al*., 1997). However, no design guidance for approach slabs is yet available in the United States (Chen and Chai, 2010; Martin and Kang, 2012).

Based on the survey results of ride comfort, different allowable slope changes for approach slabs were proposed by different researchers. Moulton (1986) suggested that slope changes of 1/250 and 1/200 would likely be tolerable for continuous and simply-supported bridges, respectively. Wahls (1990) and Stark *et al.* (1995) also believed that a slope change of 1/200 or less is acceptable from the standpoint of ride comfort. Barker *et al*. (1991), however, concluded that a gradient of 1/200 for simply-supported bridges was too conservative, and recommended a maximum allowable slope change of 1/125 to guarantee the ride comfort. Long *et al*. (1998) conducted a survey on the approaches of 1,181 bridges in Illinois and concluded that a slope change of no less than 1/100~1/125 would likely cause rider discomfort and should be proposed as a criterion for initiating remedial measures. It is not difficult to find that these recommended slope changes are inconsistent for different possible reasons. Besides relying on the survey results, Zhang and Hu (2007) carried out numerical simulations to determine the allowable slope change for approach slabs based on the ride comfort. A quarter-truck model with three degrees-of-freedom, all for vertical displacements, was adopted in their study. However, the pitching motion, which is usually more bothersome to vehicle users than the vertical motion (Bouazara and Richard, 2001), was not considered in their study.

Besides reducing the ride comfort of vehicles, slope changes in bridge approach can also reduce vehicle's running safety and accelerate the deterioration of bridge components. A slope change may cause severe vehicle vibrations and even cause the tire to lose contact with the ground, greatly reducing vehicles' operational safety and controllability (Snæbjörnsson *et al*., 2007). In addition, the impact force of the vehicle can be four to five times larger than the static vehicle load (Briaud *et al*., 1997), greatly increasing the damage to the bridge deck and other

*Research Assistant, College of Civil Engineering, Hunan University, Changsha, Hunan 410082, China (E-mail: ywchener@hnu.edu.cn)
**Professor, Key Laboratory for Wind and Bridge Engineering of Hunan Province, Hunan University, Changsha, Hunan 410082, China (Corresponding Author, E-mail: denglu@hnu.edu.cn)
***Associate Professor, School of Civil Engineering and Architecture, Changsha University of Science and Technology, Changsha, Hunan 410004, China (E-mail: yinxinfeng@163.com)

bridge components. In contrast, the current AASHTO LRFD (2012) bridge code adopts a dynamic load allowance of 0.33 for the strength design of bridge components, which may underestimate the vehicle impact due to the slope change. Based on the above discussion, it is obvious that these aspects should also be taken into consideration when suggesting a rational allowable slope change for the bridge approach slab.

To sum up, previously proposed allowable slope changes based on the survey results of the ride comfort are not consistent and limited to the geographical location where the survey was conducted while those obtained from numerical simulations were based on over-simplified vehicle models. To address these issues, in this study a three-dimensional vehicle-road-bridge interaction model is developed to study the interaction between vehicles and the road and bridge. Three typical vehicles, including cars, buses, and trucks, and a concrete box-girder bridge with approach slab are investigated. Three important indexes, namely, the tire-road contact index, the vehicle user comfort index, and the vehicle impact index, are comprehensively examined. Finally, an allowable slope change for approach slabs is suggested based on the recommended limits on the three indexes according to relevant codes including the ISO 2631 (1997) and AASHTO LRFD (2012) codes.

2. Numerical Models

A three-dimensional vehicle-road-bridge interaction model was developed to study the interaction between passing vehicles and the road (including the approach slab) and bridge. In the following sections, the bridge model, approach slab model, road surface profile, and vehicle models adopted in this study will be introduced separately in details.

2.1 Bridge Model

In this study, a typical concrete box-girder bridge with a span length of 32 m was selected according to the Segmental Box Girder Standards by the AASHTO-PCI-ASBI (1997). The bridge is a good representative of the simply-supported prestressed concrete box-girder bridges in the United States. The bridge width and the girder depth are 11.1 m and 2.4 m, respectively. Two end diaphragms with a thickness of 0.4 m are used at the ends of the bridge. Fig. 1 shows the cross section of the bridge. The selected bridge was modelled with solid elements using the ANSYS program. Each node of the solid elements has three translational degrees of freedom. A damping coefficient of 2% was assumed for all bridge vibration modes considered (Deng and Cai, 2010a). The same class of road roughness was assumed for both the approach roadway and the bridge deck.

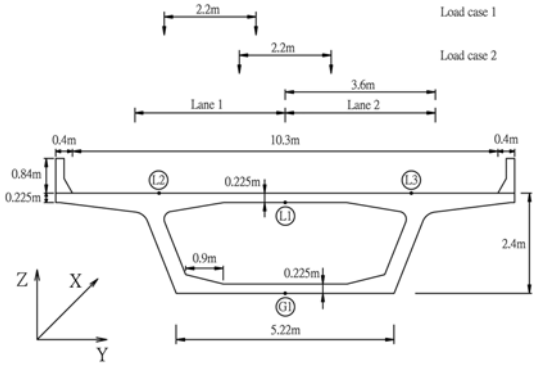

Fig. 1. Cross-section of the Bridge

2.2 Approach Slab Model

Shi *et al.* (2008) found that the deflection of an approach slab is quite small as compared to the faulting condition at the end of the approach slab, even when the faulting is relatively small. Thus, the slab deflection was not considered and the approach slab model based on the model used by Cai *et al.* (2005) was adopted in this study, as shown in Fig. 2, in which the slope change of the slab is $\theta = \Delta / L$. White *et al.* (2007) pointed out that asphalt overlay and undersealing pressure grouting operations do not help prevent further settlement or material loss at the embankment. In addition, it was found that the asphalt overlay makes a negligible change on the vehicle wheel load and therefore the vehicle impact on the bridge. Therefore, asphalt overlay was not considered in this study.

No uniform structural design guidance for approach slabs is available in the United States despite their extensive use (Chen and Chai, 2010; Martin and Kang, 2012). It is believed that the presence of approach slabs has no effect on the ultimate differential settlement that will develop between the roadway pavement and the bridge deck (Hoppe, 1999). In practice, different slab lengths may be selected to adjust the slope of the approach to the desired grade and a typical slab length is within 4-7 m (Briaud *et al*., 1997). In this study, a slab length of 6 m was

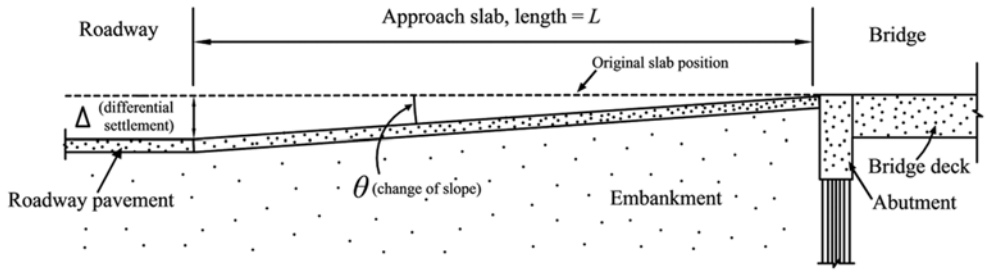

Fig. 2. Approach Slab Model

adopted. Based on a review of the common slopes of approach slabs, seven grades of slope change, namely, 1/250, 1/200, 1/150, 1/125, 1/100, 1/75 and 1/50 were investigated in this study.

2.3 Road Surface Profile

A road surface profile in numerical simulations is usually treated as a random process and can be described by a Power Spectral Density (PSD) function. A modified PSD function by Wang and Huang (1992) was adopted in this study:

$$\varphi(n) = \varphi(n_0)\left(\frac{n}{n_o}\right)^{-2} (n_1 < n < n_2) \quad (1)$$

where n is the spatial frequency (cycle/m); $\varphi(n_0)$ is the roughness coefficient (m^3/cycle) depending on the road surface condition; n_0 is the discontinuity frequency of 0.5π (cycle/m); and n_1 and n_2 are the lower and upper cutoff frequencies, respectively.

The International Organization for Standardization (ISO 1995) classifies the Road Surface Condition (RSC) based on different roughness coefficients. In the present study, very good, good, average, and poor road surface conditions corresponding to roughness coefficients of 5×10^6, 20×10^6, 80×10^6, and 256×10^6 m^3/cycle in the ISO (1995) respectively, were adopted.

Through an inverse Fourier transformation with the PSD function, the road surface profile can then be generated as follows:

$$r(X) = \sum_{k=1}^{N} \sqrt{2\varphi(n_k)\Delta n}\, \cos(2\pi n_k X + \theta_k) \quad (2)$$

where X denotes the longitudinal position of the point of interest on the road; θ_k is a random phase angle and it has a uniform distribution from 0 to 2π; and n_k is the wave number (cycle/m).

It should be pointed out that studies (ISO 1995; Cai *et al*., 2007) have shown that large irregularities, such as the differential settlements due to the slab slope change in this study, cannot be represented by a Gaussian random process and should be treated separately. In the present study, the road surface profile $r(X)$ is the superposition of the displacement due to the slope change upon the simulated random roughness profile along the roadway. A similar method was also adopted by Cai *et al.* (2007). Fig. 3 shows a segment of a good-class road surface profile including an approach slab with a length of 6 m and a slope of 1/200.

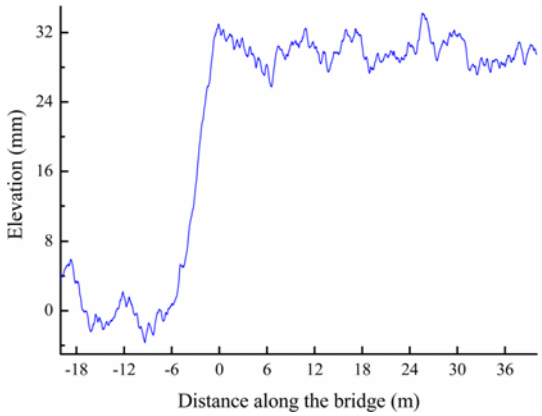

Fig. 3. A Good-class Road Surface Profile Including an Approach Slab with a Slope of 1/200

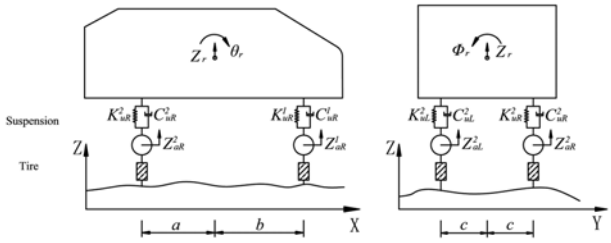

Fig. 4. Analytical Model for the Two Passenger Vehicles (see Fig. 6 for tire model)

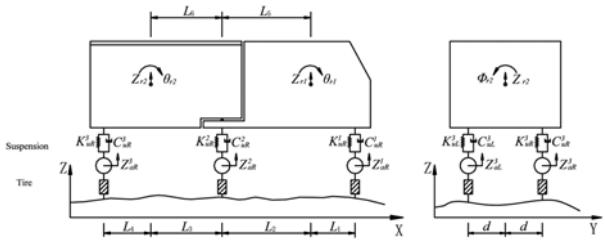

Fig. 5. Analytical Model for the Truck (see Fig. 6 for tire model)

2.4 Vehicle Models

Three typical vehicles, namely, cars, buses, and trucks, were investigated in this study. These three types of vehicles are the design vehicles used in the AASHTO (2004) code. Three-dimensional numerical models were created for all three types of vehicles. The numerical model for the two passenger vehicles, namely, the car and bus, is illustrated in Fig. 4, while the model for the truck is illustrated in Fig. 5. Detailed parameters of the vehicle models can be found in the literature (Bouazara and Richard, 2001; Deng and Cai, 2010b; Sekuliæ *et al*., 2012; Sekulić *et al*., 2013). For the readers' convenience, the primary parameters for the two passenger vehicle models and the truck model are listed in Table 1 and Table 2, respectively.

Single-point tire models have been widely adopted for vehicle tire models in the simulation of bridge-vehicle interactions due to their simplicity (Deng and Cai, 2010c; Shi *et al*., 2008; Wang and Huang, 1992). However, in reality a tire makes contact with the road surface over a footprint area instead of a single point, the use of a single-point tire model may therefore lead to amplified vibrations, especially under distressed road surface condition (Yin *et al*., 2010). Thus, a multi-point tire model proposed by Deng *et al.* (2016), as shown in Fig. 6, was adopted in this study. This tire model consists of a series of uniformly distributed points, each of which is represented by a pair of spring and damper, in contact with the road surface. The stiffness and damping coefficient values of each contact point in the multi-point tire model are therefore the values of the single-point tire model divided by the total number of contact points used. Six points were used for each tire in this study based on the

Table 1. Primary Parameters of the Passenger Vehicles under Study

Parameter	Value	
	Bus	Car
Mass of vehicle body	11,900(kg)	730(kg)
Pitching moment of inertia of vehicle body	150,000(kg·m^2)	1,230(kg·m^2)
Rolling moment of inertia of vehicle body	13,000(kg·m^2)	1,230(kg·m^2)
Mass of the front axle suspension	746(kg)	80(kg)
Upper spring stiffness of the front axle	175,000(N/m)	19,960(N/m)
Upper damper coefficient of the front axle	40,000(Ns/m)	1,290(Ns/m)
Lower spring stiffness of the front axle	1,000,000(N/m)	175,500(N/m)
Lower damper coefficient of the front axle	150(Ns/m)	0(Ns/m)
Mass of the rear axle suspension	1,355(kg)	71(kg)
Upper spring stiffness of the rear axle	408,650(N/m)	17,500(N/m)
Upper damper coefficient of the rear axle	45,973(Ns/m)	1,620(Ns/m)
Lower spring stiffness of the rear axle	2,000,000(N/m)	175,500(N/m)
Lower damper coefficient of the rear axle	150(Ns/m)	0(Ns/m)
a	2.04(m)	1.80(m)
b	3.61(m)	1.01(m)
c	1.00(m)	0.76(m)

Table 2. Primary Parameters of the Truck under Study

Parameter	Value
Mass of truck body 1	2,612 (kg)
Pitching moment of inertia of truck body 1	2,022 (kg·m^2)
Rolling moment of inertia of tuck body 1	8,544 (kg·m^2)
Mass of truck body 2	26,113 (kg)
Pitching moment of inertia of truck body 2	33,153 (kg·m^2)
Rolling moment of inertia of tuck body 2	181,216 (kg·m^2)
Mass of the first axle suspension	490 (kg)
Upper spring stiffness of the first axle	242,604 (N/m)
Upper damper coefficient of the first axle	2,190 (Ns/m)
Lower spring stiffness of the first axle	875,082 (N/m)
Lower damper coefficient of the first axle	2,000 (Ns/m)
Mass of the second axle suspension	808 (kg)
Upper spring stiffness of the second axle	1,903,172 (N/m)
Upper damper coefficient of the second axle	7,882 (Ns/m)
Lower spring stiffness of the second axle	3,503,307 (N/m)
Lower damper coefficient of the second axle	2,000 (Ns/m)
Mass of the third axle suspension	653 (kg)
Upper spring stiffness of the third axle	1,969,034 (N/m)
Upper damper coefficient of the third axle	7,182 (Ns/m)
Lower spring stiffness of the third axle	3,507,429 (N/m)
Lower damper coefficient of the third axle	2,000 (Ns/m)
L1	1.698 (m)
L2	2.569 (m)
L3	1.984 (m)
L4	2.283 (m)
L5	2.215 (m)
L6	2.338 (m)
b	1.1 (m)

suggestion by Deng *et al.* (2016). These points span a length of 25.4 cm in accordance with the AASHTO LRFD (2012) code.

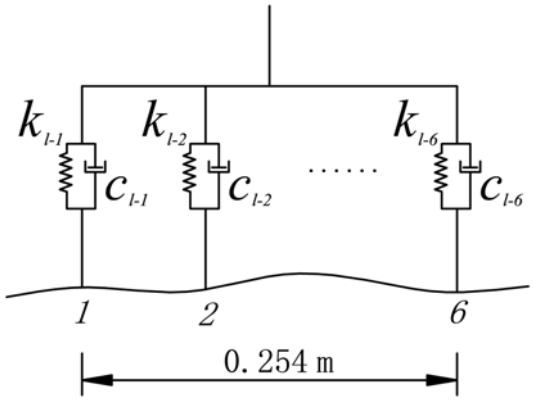

Fig. 6. Multi-point Tire Model

3. Vehicle-road-bridge Interaction System

The equation of motion for a vehicle can be expressed as follows:

$$[M_v]\{\ddot{d}_v\}+[C_v]\{\dot{d}_v\}+[K_v]\{d_v\}=\{F_G\}+\{F_v\} \quad (3)$$

where $[M_v]$, $[C_v]$, and $[K_v]$ = the mass, damping, and stiffness matrices of the vehicle, respectively; $\{d_v\}$ = the displacement vector of vehicle; $\{F_v\}$ = the wheel-road contact force vector acting on the vehicle; and $\{F_G\}$ = the gravity force vector of the vehicle.

The equation of motion for the bridge-road system can be written as follows:

$$[M_b]\{\ddot{d}_b\}+[C_b]\{\dot{d}_b\}+[K_b]\{d_b\}=\{F_b\} \quad (4)$$

where $[M_b]$, $[C_b]$, and $[K_b]$ = the mass, damping, and stiffness matrices of the bridge-road system; $\{d_b\}$ = the displacement vector of the bridge-road system; $\{F_b\}$ = the wheel-road contact

force vector acting on the road surface. It is noted that the road including the approach slab is assumed to be rigid in this study, meaning that there is no deflection in the road.

Based on the displacement relationship and interaction force relationship at the wheel-road contact points, Eqs. (3) and (4) can be combined into one coupled equation as follows:

$$\begin{bmatrix} M_b & \\ & M_v \end{bmatrix}\begin{Bmatrix} \ddot{d}_b \\ \ddot{d}_v \end{Bmatrix}+\begin{bmatrix} C_b+C_{b-b} & C_{b-v} \\ C_{v-b} & C_v \end{bmatrix}\begin{Bmatrix} \dot{d}_b \\ \dot{d}_v \end{Bmatrix} + \begin{bmatrix} K_b+K_{b-b} & K_{b-v} \\ K_{v-b} & K_v \end{bmatrix}\begin{Bmatrix} d_b \\ d_v \end{Bmatrix}=\begin{Bmatrix} F_{b-r} \\ F_{b-r}+F_G \end{Bmatrix} \tag{5}$$

where C_{b-b}, C_{b-v}, C_{v-b}, K_{b-b}, K_{b-v}, K_{v-b}, and F_{b-r} are caused by the interaction between the vehicle and the bridge-road system. As the vehicle moves, the positions of contact points change and so do these interaction terms.

Equation (5) contains the physical parameters of the vehicle-road-bridge system and solving Eq. (5) would be time consuming due to the large dimension of the matrices. The modal properties of the bridge model, including the natural frequencies and mode shapes, can be easily obtained by running a modal analysis and extracted from the ANSYS program, which can then be used to simplify the process of solving the equation of motion of the bridge model by using the modal superposition technique. Eq. (5) can then be simplified as follows:

$$\begin{bmatrix} I & \\ & M_v \end{bmatrix}\begin{Bmatrix} \ddot{\xi}_b \\ \ddot{d}_v \end{Bmatrix}+\begin{bmatrix} 2\omega_i\eta_i I+\Phi_b^T C_{b-b}\Phi_b & \Phi_b^T C_{b-v} \\ C_{v-b}\Phi_b & C_v \end{bmatrix}\begin{Bmatrix} \dot{\xi}_b \\ \dot{d}_v \end{Bmatrix} + \begin{bmatrix} \omega_i^2 I+\Phi_b^T K_{b-b}\Phi_b & \Phi_b^T K_{b-v} \\ K_{v-b}\Phi_b & K_v \end{bmatrix}\begin{Bmatrix} \xi_b \\ d_v \end{Bmatrix}=\begin{Bmatrix} \Phi_b^T F_{b-r} \\ F_{b-r}+F_G \end{Bmatrix} \tag{6}$$

where $[I]$ = unit matrix; $\{\Phi_b\}$ and $\{\xi_b\}$ are the mode shape of the bridge and the generalized modal coordinates, respectively; ω_i and η_i = the natural circular frequency and the percentage of the critical damping of the ith mode of the bridge, respectively.

Equations (6) contains only the modal information of the bridge and the mechanical parameters of the vehicles. As a result, the complexity of solving the coupled equations in Eq. (5) is greatly reduced. The fourth-order Runge-Kutta method was adopted to solve Eq. (6) in the time domain. After solving Eq. (6), the modal coordinates $\{\xi_b\}$ of the bridge model and their derivatives $\{\dot{\xi}_b\}$ and $\{\ddot{\xi}_b\}$, rather than the physical bridge responses, were obtained while the physical response of the vehicle ($\{d_v\}$, $\{\dot{d}_v\}$, and $\{\ddot{d}_v\}$) can be directly obtained. The bridge responses ($\{d_b\}$, $\{\dot{d}_b\}$, and $\{\ddot{d}_b\}$) in Eq. (4)) can then be obtained by modal decomposition. For more details of the vehicle-road-bridge interaction system, the readers can refer to Shi and Cai (2009) and Deng and Cai (2010c).

4. Evaluation Indexes

In this study, the effects of the slope change of approach slabs on three important aspects, namely, vehicle's running safety, vehicle users' comfort, and vehicle impact on the bridge, are comprehensively investigated. Three important indexes, namely, the tire-road contact index, the vehicle user comfort index, and the vehicle impact index, are used in the evaluation correspondingly.

4.1 Tire-road Contact Index

The running safety and controllability of vehicles are significantly affected by how firmly the tires contact the ground and the skid-resistance of the road surface. In situations such as icy and wet roads and bumps, vehicle tires may have loose contact with the road surface, leading to poor vehicle controllability and potential safety issues. A tire-road contact index, which is defined as the ratio between the minimum dynamic wheel load and the static wheel load, was used in this study to measure how firmly vehicle tires contact the ground.

4.2 Vehicle User Comfort Index

The comfort level for the passenger vehicles, namely, the car and bus, was analyzed. According to the evaluation method for the vehicle users' comfort adopted by Sekulić *et al*. (2013), the acceleration of the vehicle in certain location can reflect the comfort level of the user sitting in the corresponding location. Thus, in this paper the accelerations of both the driver and passengers were studied for the car, and the accelerations of the driver and passengers at the middle ("passenger_mid" for short) and rear overhand ("passenger_rear" for short) of the bus were studied for the bus.

In this study, two load cases were adopted for vehicle loading in which a single vehicle was set to travel along the centerline of Lane 1 and the centerline of the deck slab respectively, as shown in Fig. 1. Fig. 7 plots the vehicle users' vertical acceleration for both the car and bus under the two load cases in which each vehicle was set to pass through a slope change of 1/150 at a speed of 100 km/h. It should be noted that the acceleration of the bus rear passengers is not plotted in Fig. 7(b) in order to make the figure more readable.

Figure 7 shows that the acceleration peak induced by the slope change attenuates very quickly and the total duration is much less than one minute. The ISO 2631 (1997) suggests that the running root-mean-square (RMS) acceleration, as defined by Eq. (7), should be used to evaluate the human comfort under vibrations that have durations of less than one minute, such as the transient vibration, and recommends the use of one second as the integration time when calculating the running RMS value.

$$a_\omega(t_0)=\left\{\frac{1}{\tau}\int_{t_0-\tau}^{t_0}[a_\omega(t)]^2 dt\right\}^{\frac{1}{2}} \tag{7}$$

where $a_\omega(t)$ is the instantaneous frequency-weighted acceleration; τ is the integration time for the running average; t is the time; and t_0 is the instantaneous time point. It should be noted that the frequency range considered for comfort is from 0.5 Hz to 80 Hz. Therefore, $a_\omega(t)$ was obtained from the acceleration, which can

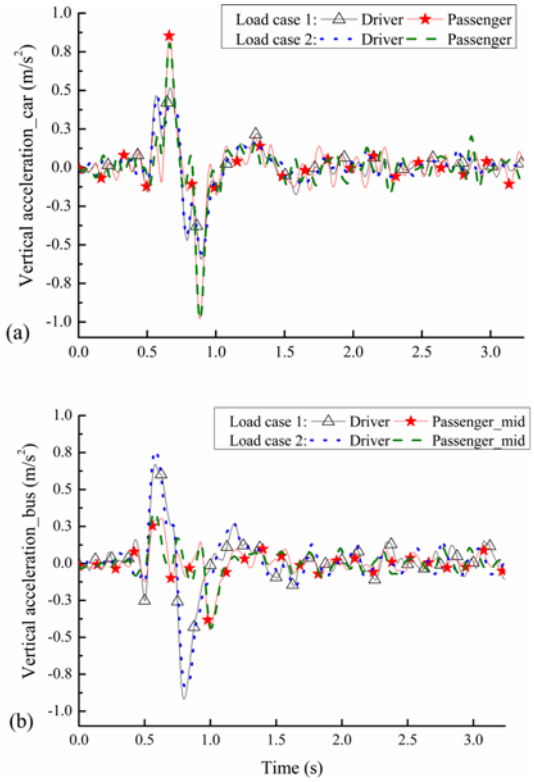

Fig. 7. Vehicle Users' Vertical Acceleration under the Two Load Cases: (a) Car, (b) Bus

Table 3. Comfort Reactions to Vibration Environments

MTVV (m/s²)	Degree of comfort
<0.315	Not uncomfortable
0.315~0.63	Little uncomfortable
0.50~1.00	Fairly uncomfortable
0.80~1.60	Uncomfortable
1.25~2.5	Very uncomfortable
>2.00	Extremely uncomfortable

be derived from $\{\ddot{d}_v\}$ in Eq. (6), by using a band-limiting filter with a high pass frequency of 0.5 Hz and low pass frequency of 80 Hz.

It was found that varying the integration time can result in a considerable variation of the running RMS values (Lewis and Griffin, 1998). In this regard, a term named maximum transient vibration value (MTVV) is defined in the ISO 2631 (1997) as the highest magnitude of the running RMS obtained during the measurement period, as defined as Eq. (8).

$$\text{MTVV} = \max[a_w(t_0)] \tag{8}$$

Eventually, the vehicle user comfort index was reflected by the values of the MTVV. Table 3 summarizes the likely comfort reactions to vibrations of various magnitudes according to the ISO 2631 (1997) code.

4.3 Vehicle Impact Index

Studies have shown that the dynamic wheel loads induced by a bump can be 4-5 times larger than the static wheel loads, and can greatly increase the damage to the bridge deck (Hoppe, 1999; Briaud *et al.*, 1997). In the bridge design codes, the impact factor (IM) is usually used to evaluate the vehicle impact on the bridge. The impact factors defined in the bridge codes (see Eq. (9)), for both bridge girder and deck, are traditionally derived from the global responses of the bridge, i.e., the global bending moment or vertical deflection at the mid-span of the girder (Hwang and Nowak, 1991; AASHTO LRFD 1994). In fact, for the bridge deck, the transverse bending moment is, in most cases, the controlling internal force in design. Therefore, using the IMs based on the global bridge responses to evaluate the local impact on the bridge deck may be unreasonable. In order to differentiate the vehicle impact on the bridge deck and that on the bridge girder, the concept of local impact factor, which is calculated from the transverse bending strain of the deck, is proposed as compared to the global impact factor calculated from the longitudinal bending strain of the girder at mid-span in the following analysis. The vehicle impact index in the present study was therefore evaluated by the values of the local IM and global IM. It should be noted that only the truck impact on the bridge was analyzed in this study. The impact factor is defined as follows:

$$IM = \frac{R_{dyn} - R_{sta}}{R_{sta}} \tag{9}$$

where R_{dyn} and R_{sta} are the maximum dynamic and static responses of the target point on the bridge, respectively.

Figure 1 shows the points of interest, marked as L1, L2 and L3, used for calculating the local IMs of the deck slab and the point for calculating the global IM of the bridge, which is marked as G1. Since the local transverse bending moment at L2 is certainly no less than that at L3 under both load cases, only L2 was investigated. Eventually, L1 and L2 were selected as the points of interest for investigating the positive and negative transverse bending moments of the deck slab and the local impact factors, while G1 was selected for investigating the global bending moment of the girder and the global impact factor.

Points or cross sections that have the largest static responses should be selected for investigating the impact factor. The point G1 for studying the global impact factor is located at the mid-span of the main girder. The static longitudinal strains at G1 under Load case 1 and Load case 2 are 17.6 μ and 17.3 μ, respectively. To determine the longitudinal positions of the points L1 and L2 on the bridge, quasi-static analysis was performed for both load cases in which the truck moved across the bridge step by step, and the static transverse strains at L1 and L2 at each step were recorded. Then, the longitudinal positions at which the maximum static strains occurred were selected for calculating the local impact factors. Table 4 shows the maximum static transverse strains and the corresponding positions of the points selected for calculating the local impact factors.

It should be noted that only the uphill case was considered in this study, i.e., the vehicle passes through the slope change in

Table 4. Maximum Static Transverse Strains and Corresponding Longitudinal Positions of the Points L1 and L2 under the Two Load Cases

Point of interest	Load case 1		Load case 2	
	Distance to bridge end (m)	Static strain (μ)	Distance to bridge end (m)	Static strain (μ)
L1	3.2	13.46	3.2	19.07
L2	3.2	6.91	3.0	7.93

Fig. 2 from left to right. Zhang and Hu (2007) have shown that the driving direction has little effect on the vehicle user's MTVV values and the maximum vertical wheel force when the vehicle travels through a downhill or uphill section. Meanwhile, due to the fact that the elevation of bridge deck is higher than that of the road section, in the downhill case larger vehicle impact will occur on the approach slab and road section due to the vehicle oscillation induced by the slope change rather than on the bridge deck while in the uphill case larger vehicle impact will occur on the bridge deck. As a result, the vehicle impact on the bridge deck in the uphill case is very likely greater than that in the downhill case, and therefore there is no need to consider the downhill case. Based on these reasons, it is not necessary to consider the downhill case in this study.

5. Parametric Analysis

In the present study, seven grades of slope change were investigated, namely 1/250, 1/200, 1/150, 1/125, 1/100, 1/75, and 1/50. Six vehicle speeds ranging from 20 km/h to 120 km/h, with intervals of 20 km/h, were considered. Four road surface conditions according to the ISO (1995) were studied, namely, very good, good, average, and poor. Three important indexes, namely, the tire-road contact index, the vehicle user comfort index, and the vehicle impact index were investigated. A series of cases were studied with different combinations of loading position, vehicle speed, road surface condition, and slab slope change. Under each specific case, the vehicle-road-bridge interaction analysis program was set to run 20 times with 20 sets of randomly generated road surface profiles under the given road surface condition. As a result, each of the indexes was calculated 20 times for a specific case, and the averages of the 20 values were then used in the result analysis.

5.1 Effect of Loading Condition

Figure 8 shows the time histories of the front wheel loads of the car, bus, and truck for the two load cases when the vehicles travel at 100 km/h through the bridge approach with a slope change of 1/150. It should be noted that the wheel loads in the figure are standardized values, which are equal to the dynamic wheel loads divided by the corresponding static wheel loads, so that the magnitude of the dynamic effect is more straightforward. As a result, the tire-road contact index can be directly obtained as the minimum standardized wheel load.

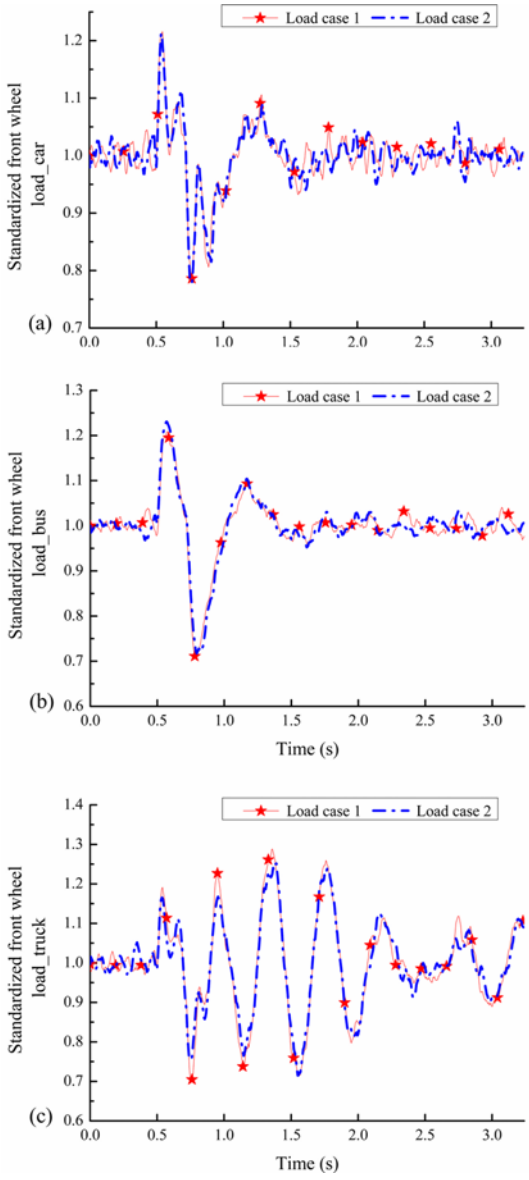

Fig. 8. Time Histories of the Standardized Front Wheel Loads under the Two Load Cases: (a) Car, (b) Bus, (c) Truck

As can be seen from Figs. 7 and 8, the differences in the passenger vertical acceleration and the wheel load between the two load cases are very small. Thus, it is sufficient to consider the tire-road contact index and vehicle user comfort index under either of the two load cases, and Load case 2 was adopted in the following analysis. However, the static longitudinal strain at G1 under Load case 1 is slightly larger than that under Load case 2. Therefore, both load cases were considered when investigating vehicle's impact on the bridge.

5.2 Effect of Vehicle Speed

To investigate the effect of vehicle speed on the evaluation indexes, the vehicles were set to pass through the bridge approach with different slope changes at different speeds from 20 km/h to 120 km/h. Figs. 9 and 10 plot the tire-road contact indexes and

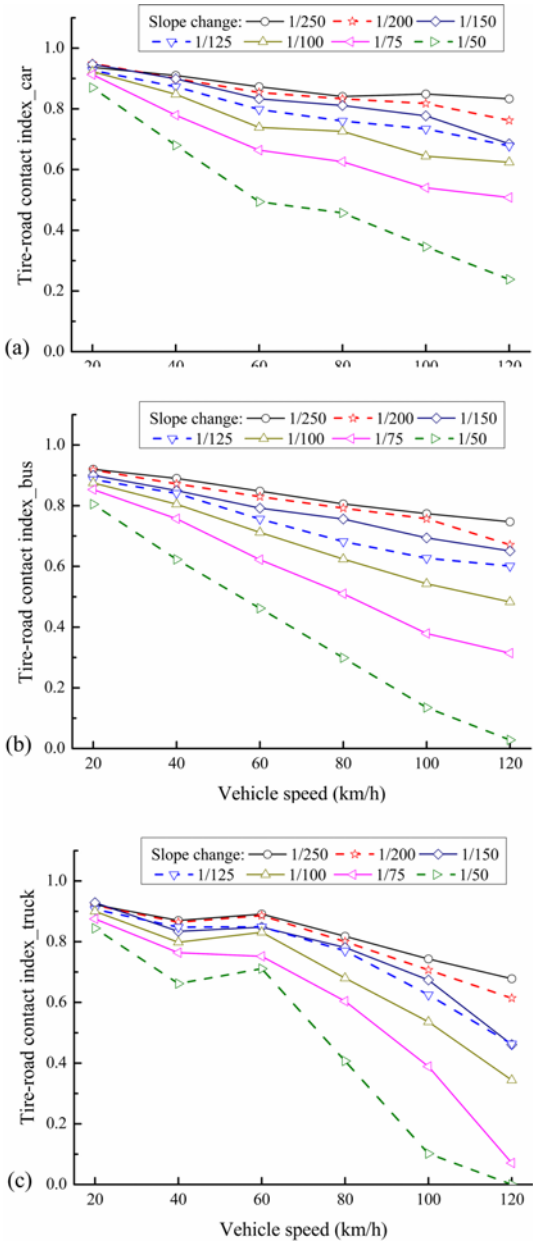

Fig. 9. Effect of Vehicle Speed on the Tire-road Contact Index: (a) Car, (b) Bus, (c) Truck

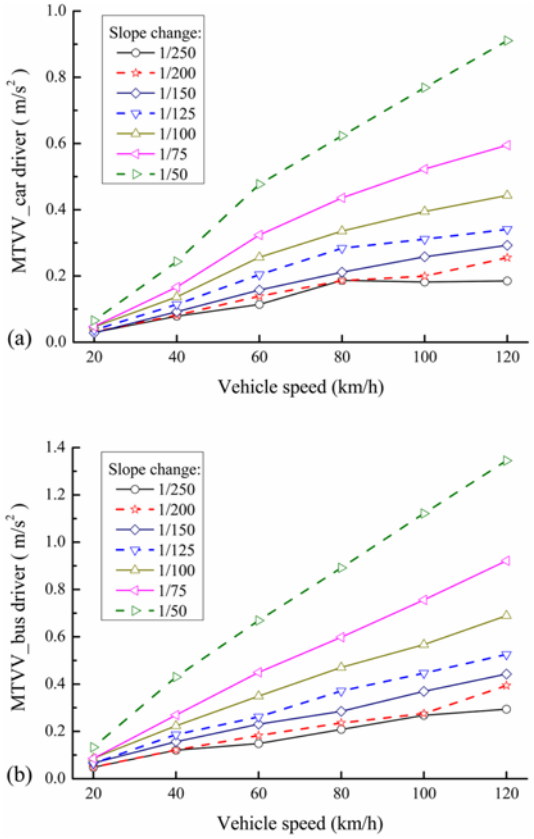

Fig. 10. Effect of Vehicle Speed on Driver's MTVV: (a) Car, (b) Bus

the driver's MTVV values, respectively, for all the cases considered. It should be noted that in these two figures averaged results for all four RSCs considered are used. As shown in Fig. 9, the tire-road contact index tends to decrease with the increase of vehicle speed, and this tendency becomes more significant with the increase of the slope change. For the bus and truck, the tire-road contact index can get close to or even reach zero at a slope change of 1/50, indicating that the vehicle tire may totally lose contact with the road surface.

From Fig. 10, it can be easily observed that the driver's MTVV increases almost linearly with the increase of vehicle speed, resulting in a decrease in the driver's comfort level. In addition, similar to the cross influence of vehicle speed and slope change on the tire-road contact index, the influence of vehicle speed on the driver's MTVV becomes more significant as the slope change increases. It is also noted that at relatively high vehicle speed (no less than 80 km/h), the driver's MTVV value can well exceed the threshold value, i.e., 0.315 m/s^2 as listed in Table 3, for feeling comfortable under slope changes greater than 1/125.

The impact factors, both global and local, are also plotted against vehicle speed, as shown in Fig. 11. It should be noted that in this figure averaged results for all four RSCs and seven slope changes considered are used. It is emphasized again that the local impact factors are calculated based on the transverse bending strains at points L1 and L2 at specific cross sections and the global impact factors are calculated based on the longitudinal bending strain at point G1 which is at the bottom of the midspan of the girder. It can be observed that the variation of both the local and global IMs do not follow a certain trend with the change of vehicle speed. Similar phenomenon has also been observed in other studies (Broquet *et al*., 2004; Deng and Cai, 2010b; Green *et al.,* 1995). In fact, the effect of vehicle speed on impact factor is a very complex issue in that it is affected simultaneously by many other factors (Deng *et al*., 2015). Unfortunately no consensus on the explanation has yet been reached despite the attempt by many researchers.

From Fig. 11, it can also be easily seen that the global and local IMs are not identical and that the vehicle speed influences the global and local IMs in different ways, especially when the

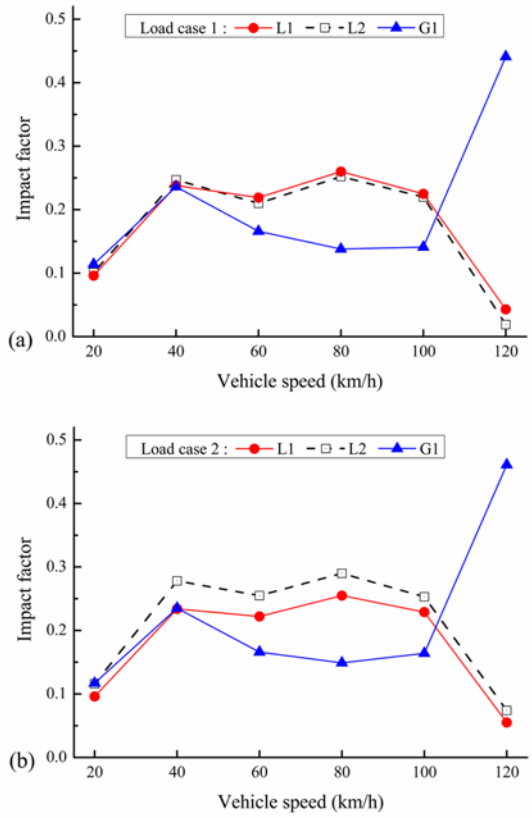

Fig. 11. Effect of Vehicle Speed on Impact Factors under the Two Load Cases: (a) Load Case 1, (b) Load Case 2

vehicle speed is in the range of 60 km/h to 120 km/h. Huang (2013) also found that the vehicle-induced local vibration of the bridge deck is quite different from the global vibration of the main girder.

5.3 Effect of Road Surface Condition

Road surface will experience progressive deterioration under the effect of natural erosion and repeated vehicle loading. The simulated tire-road contact indexes for each vehicle are plotted against the road surface condition, as shown in Fig. 12, where the tire-road contact index at each speed under each slab slope change is the average value for the six different speeds. From the figure, it can be clearly seen that the tire-road contact index for each vehicle reduces notably as the slope change increases. However, the effect of road surface condition on the tire-road contact index is not as significant as that of the slope change. Particularly, the effect of road surface condition on the tire-road contact index is insignificant when the slope change reaches 1/50.

Figure 13 shows the driver's MTVV values obtained under the four road surface conditions. It should be noted that in this figure averaged results for all six speeds are used. Similar to the observations made in Fig. 12, the driver's MTVV values for both vehicle types increase significantly with the increase of slope change while the effect of road surface condition on the driver's MTVV is less significant than that of the slope change, especially under relatively large slope changes. It can be easily observed

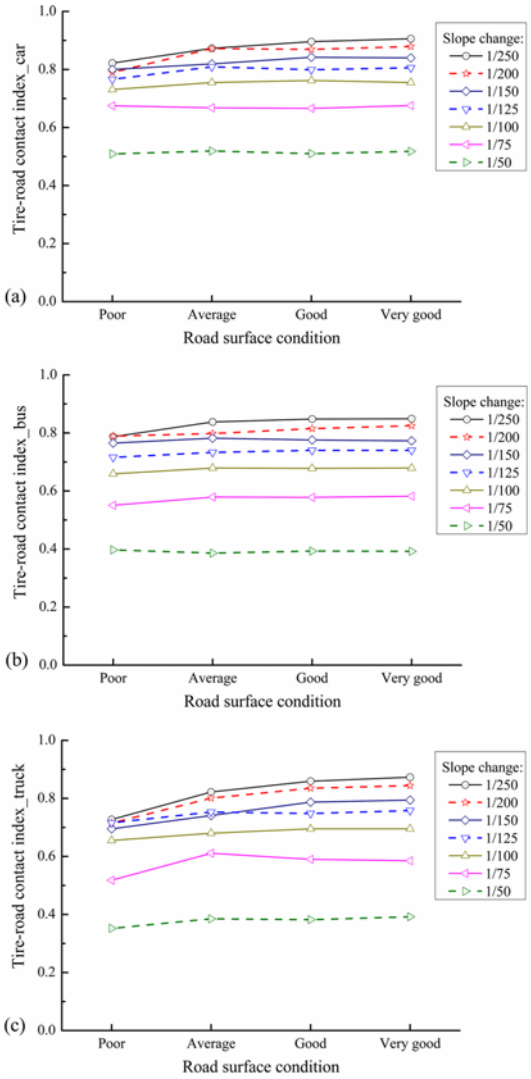

Fig. 12. Effect of the Road Roughness on the Tire-road Contact Index: (a) Car, (b) Bus, (c) Truck

that when the slope change is no larger than 1/125, the driver's MTVV values generally fall below 0.315 m/s^2, indicating that the drivers will not feel uncomfortable. However, the MTVV values of the car driver and bus driver can reach 0.52 m/s^2 and 0.78 m/s^2, respectively, under a slope change of 1/50 despite the road surface condition, implying that under large slope changes the drivers will feel uncomfortable to different degrees even when the road surface condition is good.

Figure 14 shows the variation of the average global and local IMs with the road surface condition under the two load cases, where the impact factors were obtained for seven slab slope changes while considering all vehicle speeds. It can be observed that both the global and local IMs decrease as the road surface condition improves. It is also noted that the local IMs are larger than the global IM under poor road surface condition; however, the local IMs are generally smaller than the global IM under average or better road surface conditions. This phenomenon may indicate that the local impact factors are more sensitive to the

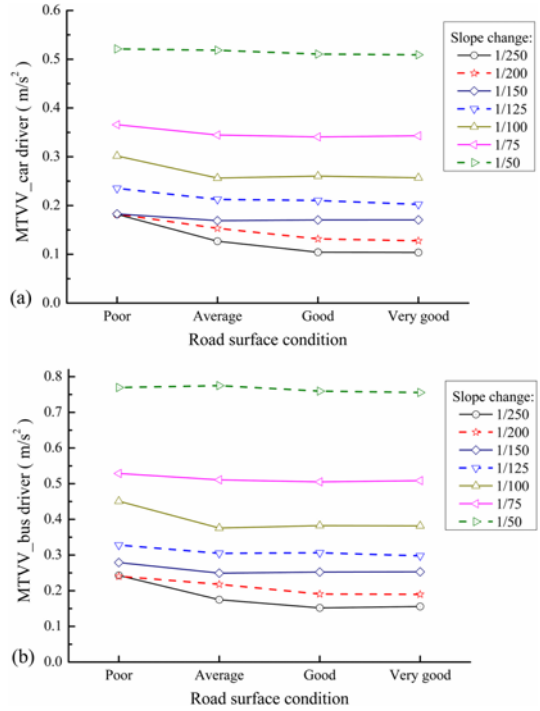

Fig. 13. Effect of the Road Roughness on Driver's MTVV: (a) Car, (b) Bus

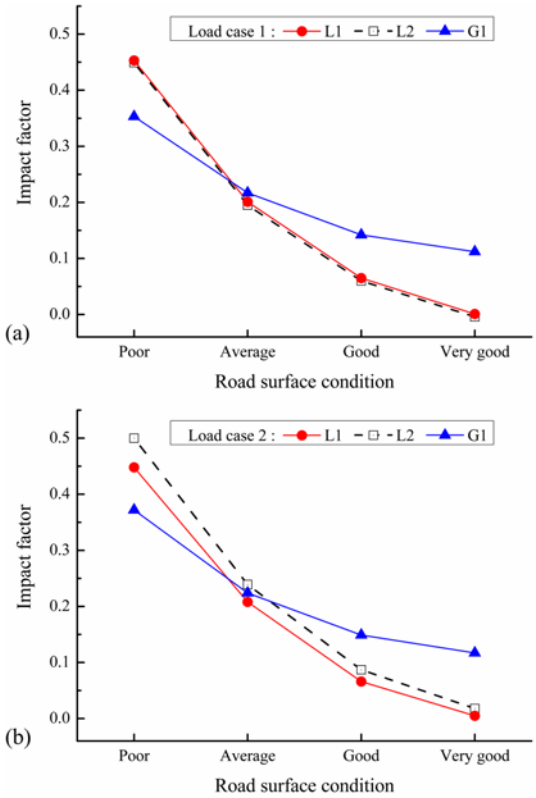

Fig. 14. Effect of the Road Roughness on Impact Factors under the Two Load Cases: (a) Load Case 1, (b) Load Case 2

road roughness than the global impact factors. This could be explained by the fact that the local dynamic response is dominated by the local vibration modes of the bridge deck which are easily excited by the dynamic wheel loads that are largely affected by the road roughness, while the global dynamic response is largely affected by the first few (especially the first) vertical bending modes of the bridge. As a result, the road roughness has a more direct influence on the local vibration mode and therefore the local impact factors than on the global impact factors.

6. Determination of the Allowable Slope Change

Before conducting parametric studies to determine the allowable slope change, reasonable assumptions need to be made for some parameters. Under normal operational condition, pavement can maintain a "good" condition for two-thirds of its expected service life (Zhang and Cai, 2011). Therefore, a good road surface condition was therefore adopted. In addition, from the previous analysis it can be found that vehicle speed and slope change have a significant cross influence on the three indexes investigated. Typically, the 85th percentile speed is used by many states and cities for establishing regulatory speed zones, and is usually adopted as the critical speed in parametric studies. In this study, a speed of 100 km/h was adopted as the critical speed based on the reference speed of 26.8 m/s recommended by Zhang and Cai (2011).

6.1 Allowable Slope Change Based on the Tire-road Contact Index

The running safety of vehicles is significantly affected by how firmly vehicle tires contact the ground. The tire-road contact index is a good measure of how firmly the tire contacts the

Table 5. Tire-road Contact Index of Vehicles under Different Slope Changes

Case description	Slope change	Car		Bus		Truck		
		Front wheel	Rear wheel	Front wheel	Rear wheel	Front wheel	Middle wheel	Rear wheel
Load case 2; Good RSC; Vehicle speed = 100 km/h	1/250	0.867	0.767	0.861	0.911	0.826	0.875	0.853
	1/200	0.851	0.737	0.794	0.863	0.785	0.855	0.816
	1/150	0.778	0.601	0.717	0.797	0.715	0.797	0.751
	1/125	0.736	0.523	0.669	0.782	0.642	0.759	0.689
	1/100	0.65	0.371	0.568	0.689	0.553	0.724	0.630
	1/75	0.545	0.194	0.428	0.601	0.384	0.583	0.443
	1/50	0.348	0.011	0.146	0.407	0.090	0.500	0.279

ground. The tire-road contact indexes, for both the front and rear wheels, of the car, bus, and truck, when the vehicles passing different slope changes are summarized in Table 5. As can be seen from the table, the tire-road contact indexes for all three vehicles considered, for both the front and rear wheels, are greater than zero under all slope changes considered. This indicates that for the range of slope changes under consideration, the vehicle's running safety may not be the controlling factor for determining the allowable maximum slope change of the approach slab.

6.2 Allowable Slope Change Based on the Vehicle User Comfort Index

Vehicle vibration induced by the slope change at the bridge approach will reduce vehicle users' comfort. A rational threshold value for the slope change should balance the need of the vehicle users' comfort and the construction and maintenance cost for controlling the slope change under the desired level. Cantisani and Loprencipe (2010) studied the relationship between vehicle users' comfort and the vertical acceleration, which is equal to the MTVV in this case, and they concluded that with a vertical acceleration within the range of 0.315~0.63 m/s^2 vehicle users would only feel "little uncomfortable". The ISO 2631 (1997) adopts the same range of 0.315~0.63 m/s^2 for the MTVV value as the "little uncomfortable" zone for vehicle users, as shown in Table 3. Vehicle users will feel "fairly uncomfortable" when the MTVV value is beyond this range. Therefore, a MTVV value of 0.63 m/s^2 was adopted as the threshold value for maintaining a desired level of comfort for vehicle users in this study.

The MTVV values for the car and bus users obtained under the seven grades of slope change are summarized in Table 6. Based on the threshold value of 0.63 m/s^2, it can be obtained from Table 6 that the maximum slope change of the approach slab which satisfies the comfort requirements of the users of both vehicle types is 1/100.

6.3 Allowable Slope Change Based on the Vehicle Impact Index

The global and local impact factors under the seven slope changes for both Load case 1 and Load case 2 are listed in Table 7. From Table 7 it can be seen that for the two load cases considered, the global and local impact factors under the seven slope changes considered are all smaller than the specified IM of 0.33 by the AASHTO LRFD (2012) code. It is also observed that the global impact factors increase as the slope change increases while the variation of the local impact factors do not follow a similar trend.

To further examine the relationship between the local impact factor and the slope change of approach slab, by assuming a smooth road surface profile, the local impact factors at points L1 and L2 when the truck passes through different slope changes under Load case 2 were obtained, as shown in Fig. 15. The purpose of assuming a smooth road surface is to eliminate the disturbance brought by the random road roughness and to focus on the effect of slope change on the local IMs. In addition, an additional slope change of 1/25 was also considered in order to obtain a clearer variation tendency of the local impact factor with respect to the slope change.

From Fig. 15 it can be seen that the local impact factors are very small and they vary slowly with the increase of the slope change of the approach slab when the slope change is no greater than 1/100. However, when the slope change increases from 1/100 to 1/25, the local impact factors increase much faster and the trend becomes more significantly with the increase of slope

Table 6. MTVV of Passenger Vehicles undeR Different Slope Changes

Case description	Slope change	Car		Bus		
		Driver	Passenger	Driver	Passenger_mid	Passenger_rear
Load case 2; Good RSC; Vehicle speed = 100 km/h	1/250	0.145	0.134	0.207	0.097	0.206
	1/200	0.188	0.176	0.263	0.115	0.257
	1/150	0.257	0.243	0.368	0.155	0.354
	1/125	0.318	0.299	0.452	0.181	0.429
	1/100	0.392	0.371	0.552	0.233	0.540
	1/75	0.515	0.483	0.732	0.305	0.712
	1/50	0.767	0.724	1.105	0.462	1.075

Table 7. Impact factors of the truck under different slope changes

Case description	Slope change	Load case 1			Load case 2		
		L1	L2	G1	L1	L2	G1
Good RSC; Vehicle speed= 100 km/h	1/250	0.114	0.109	0.016	0.116	0.141	0.022
	1/200	0.104	0.104	0.019	0.107	0.127	0.022
	1/150	0.065	0.057	0.021	0.094	0.112	0.034
	1/125	0.084	0.066	0.033	0.060	0.072	0.047
	1/100	0.079	0.058	0.061	0.069	0.068	0.094
	1/75	0.069	0.053	0.130	0.056	0.051	0.164
	1/50	0.048	0.031	0.292	0.083	0.068	0.302

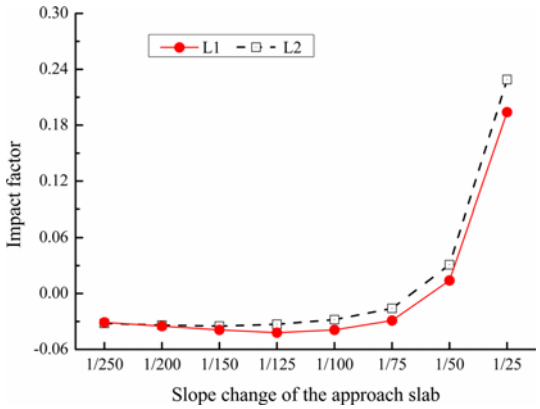

Fig. 15. The Local Impact Factors at Points L1 and L2 under Different Slope Changes

change. Furthermore, based on a comparison between the results of local impact factors in Fig. 15 and those summarized in Table 7, it can be found that the presence of road roughness does lead to an increase in the local impact factors over those under a smooth road surface as the local IMs in Table 7 are all larger than the corresponding IMs in Fig. 15.

It can also be observed from Table 7 that the local impact factors are all smaller than 0.15 while the largest global impact factor can reach 0.3. Similar phenomenon was also observed by other researchers (Huang *et al.*, 1993; Huang, 2013). The current AASHTO LRFD (2012) code employs a single value of 0.33 for the impact factor and does not differentiate it between the global design of bridge girders and the local design of bridge deck. In fact, the impact factors in many design codes were traditionally derived from global bridge responses. For instance, the impact provision in the AASHTO LRFD (1994) code was based on the work by Hwang and Nowak (1991) in which the deflection at the bridge mid-span was used to calculate the impact factors. However, the applicability of the global impact factor to the local design of bridge decks has not been justified. Based on the findings from this study and Yu *et al.* (2015), it is therefore suggested that the impact factors used for the design of bridge deck and girder may need to be treated differently.

In addition, it can be observed from Fig. 15 that in some cases negative local impact factors are obtained. Similar results have also been observed by Huang (2013). The main reason for this could be that the influence zone on the bridge deck, in the bridge longitudinal direction, that affect the deck transverse moment is relatively narrow while the effective excitation time of the vehicle load on the bridge deck is very short (Huang, 2013).

Based on the results in the previous three sub-sections, it can be found that the threshold values of the slope change that can satisfy the requirements of all three aspects, namely, vehicle's running safety, vehicle users' comfort, and vehicle impact on the bridge, are determined to be 1/50, 1/100, and 1/50, respectively. Therefore, vehicle users' comfort is the controlling factor, among all the three factors considered, for determining the maximum allowable slope change for the bridge approach. Based on these results, a slope change of 1/100 can be adopted as the maximum allowable slope change of the approach slab.

7. Conclusions

In this study, a three-dimensional vehicle-road-bridge interaction model was developed to study the interaction between vehicles and the road and bridge. Scenarios in which three typical vehicles, including cars, buses, and trucks, pass through the slope change at the approach of a concrete box-girder bridge were investigated. Three important indexes, namely, the tire-road contact index, the vehicle user comfort index, and the vehicle impact index were examined. It was found that the vehicle users' comfort is the controlling factor, among all three factors considered, in determining the maximum allowable slope change. Based on the recommended limits on the three indexes according to the ISO 2631 (1997) and AASHTO LRFD (2012) codes, a slope change of 1/100 is proposed as the maximum allowable slope change of approach slabs. A parametric study was also conducted to investigate the effects of a few important parameters on the three evaluation indexes, and the following conclusions can be drawn:

The increase of both the vehicle speed and slope change of the approach slab will lead to a reduction of the tire-road contact index, reducing the running safety and controllability of vehicles.

The comfort of passenger vehicle users will improve as the vehicle speed decreases or the slope change of the approach slab reduces.

The slope change of the approach slab has a much more significant effect on the tire-road contact index and the comfort of passenger vehicle users than the road surface condition.

Both the global and local impact factors decrease significantly as the road surface condition improves, and the local impact factor is more sensitive to the road roughness than the global impact factor. In addition, the large difference in the global and local impact factors indicates that they may need to be treated differently in practice.

Acknowledgements

The authors gratefully acknowledge the financial support provided by the National Natural Science Foundation of China (Grant No. 51208189 and 51478176) and Excellent Youth Foundation of Hunan Scientific Committee (Grant No. 14JJ1014).

References

American Association of State Highway and Transportation Officials (AASHTO) (2004). *A Policy on geometric design of highways and streets*, Washington, DC.

American Association of State Highway and Transportation Officials (AASHTO) (1994). *LRFD bridge design specifications,* Washington, DC.

American Association of State Highway and Transportation Officials (AASHTO) (2012). *LRFD bridge design specifications,* Washington,

DC.

American Association of State Highway and Transportation Officials-Precast/Prestressed Concrete Institute-American Segmental Bridge Institute (AASHTO–PCI–ASBI) (1997). Segmental box girder standards. Washington, DC.

Barker, R. M., Duncan, J., Rojiani, K., Ooi, P., Tan, C., and Kim, S. (1991). *Manuals for the design of bridge foundations: Shallow foundations, driven piles, retaining walls and abutments, drilled shafts, estimating tolerable movements, and load factor design specifications and commentar*y, NCHRP Rep. No. 343, TRB, National Research Council, Washington, D.C.

Bouazara, M. and Richard, M. J. (2001). "An optimization method designed to improve 3-D vehicle comfort and road holding capability through the use of active and semi-active suspensions." *European Journal of Mechanics-A/Solids*, Vol. 20, No. 3, pp. 509-520, DOI: 10.1016/S0997-7538(01)01138-X.

Briaud, J. L., Maher, S. F., and James, R. W. (1997). "Bump at the end of the bridge." *Civil Engineering—ASCE*, Vol. 67, No. 5, pp. 68-69.

Broquet, C., Bailey, S. F., Fafard, M., and Brühwiler, E. (2004). "Dynamic behavior of deck slabs of concrete road bridges." *Journal of Bridge Engineering*, Vol. 9, No. 2, pp. 137-146, DOI: 10.1061/(ASCE) 1084-0702(2004)9:2(137).

Cai, C., Shi, X., Voyiadjis, G., and Zhang, Z. (2005). "Structural performance of bridge approach slabs under given embankment settlement." *Journal of Bridge Engineering*, Vol. 10, No. 4, pp. 482-489, DOI: 10.1061/(ASCE)1084-0702(2005)10:4(482).

Cai C. S., Shi X. M., Araujo M., and Chen S. R. (2007). "Effect of approach span condition on vehicle-induced dynamic response of slab-on-girder road bridges." *Engineering Structures*, Vol. 29, No. 12, pp. 3210-3226, DOI: 10.1016/j.engstruct.2007.10.004.

Cantisani, G. and Loprencipe, G. (2010). "Road roughness and whole body vibration: Evaluation tools and comfort limits." *Journal of Transportation Engineering*, Vol. 136, No. 9, pp. 818-826, DOI: 10.1061/(ASCE)TE.1943-5436.0000143.

Chen, Y. T. and Chai, Y. (2010). "Experimental study on the performance of approach slabs under deteriorating soil washout conditions." *Journal of Bridge Engineering*, Vol. 16, No. 5, pp. 624-632, DOI: 10.1061/(ASCE)BE.1943-5592.0000188.

Deng, L. and Cai, C. S. (2010a). "Bridge model updating using response surface method and genetic algorithm." *Journal of Bridge Engineering*, Vol. 15, No. 5, pp. 553-564, DOI: 10.1061/(ASCE)BE.1943-5592.0000092.

Deng, L. and Cai, C. (2010b). "Development of dynamic impact factor for performance evaluation of existing multi-girder concrete bridges." *Engineering Structures*, Vol. 32, No. 1, pp. 21-31, DOI: 10.1016/j.engstruct.2009.08.013.

Deng, L. and Cai, C. (2010c). "Identification of dynamic vehicular axle loads: theory and simulations." *Journal of Vibration and Control*, Vol. 16, No. 14, pp. 2167-2194, DOI: 10.1177/1077546309351221.

Deng, L., Yu, Y., Zou, Q., and Cai, C. (2015). "State-of-the-art review of dynamic impact factors of highway bridges." *Journal of Bridge Engineering*, Vol. 20, No. 5, 04014080, DOI: 10.1061/(ASCE)BE.1943-5592.0000672.

Deng, L., Cao, R., Wang, W., and Yin, X. (2016). "A multi-point tire model for studying bridge-vehicle coupled vibration." *International Journal of Structural Stability and Dynamics*, Vol. 14, No. 4, DOI: 10.1142/S0219455415500479.

Green, M. F., Cebon, D., and Cole, D. J. (1995). "Effects of vehicle suspension design on dynamics of highway bridges." *Journal of Structural Engineering*, Vol. 121, No. 2, pp. 272-282, DOI: 10.1061/(ASCE)0733-9445(1995)121:2(272).

Hoppe, E. J. (1999). *Guidelines for the use, design, and construction of bridge approach slabs*, Rep. No. VTRC 00-04, Virginia Transportation Research Council, Charlottesville, Va.

Huang, D. (2013). *Impact behavior of concrete bridge deck on girders due to moving vehicles*, Proc., Structures Congress 2013: Bridging Your Passion with Your Profession, ASCE, Pittsburgh, PA, pp. 689-698, DOI: 10.1061/9780784412848.061.

Huang, D. Z., Wang, T. L., and Shahawy, M. (1993). "Impact studies of multigirder concrete Bridges." *Journal of Structural Engineering*, Vol. 119, No. 8, pp. 2387-2402, DOI: 10.1061/(ASCE)0733-9445 (1993)119:8(2387).

Hwang, E. S. and Nowak, A. S. (1991). "Simulation of dynamic load for bridges." *Journal of Structural Engineering*, Vol. 117, No. 5, pp. 1413-1434, DOI: 10.1061/(ASCE)0733-9445(1991)117:5(1413).

International Organization for Standardization (ISO) (1995). *Mechanical vibration-road surface profiles-reporting of measured data*, ISO 8068: (E), Geneva.

International Organization for Standardization (ISO) (1997). *Mechanical vibration and shock-Evaluation of human exposure to whole body vibration-Part1: General requirements*, ISO 2631-1:1997E, Geneva.

Lewis, C. and Griffin, M. (1998). "A comparison of evaluations and assessments obtained using alternative standards for predicting the hazards of whole-body vibration and repeated shocks." *Journal of Sound and Vibration*, Vol. 215, No. 4, pp. 915-926, DOI: 10.1006/jsvi.1998.1591.

Long, J. H., Olson, S. M., Stark, T. D., and Samara, E. A. (1998). "Differential movement at embankment-bridge structure interface in Illinois." *Transportation Research Record: Journal of the Transportation Research Board*, Vol. 1633, No. 1, pp. 53-60, DOI: 10.3141/1633-07.

Martin, R. D. and Kang, T. H. K. (2012). "Structural design and construction issues of approach slabs." *Practice Periodical on Structural Design and Construction*, Vol. 18, No. 1, pp. 12-20, DOI: 10.1061/(ASCE)SC.1943-5576.0000133.

Moulton, L. K. (1986). *Tolerable movement criteria for highway bridge*, Final Rep. No. FHWA-TS-85-228, Federal Highway Administration, Washington, D.C.

Sekulić, D., Dedović, V., and Rusov, S. (2012). "Effect of shock vibrations due to speed control humps to the health of city bus drivers." *Scientific Research and Essays*, Vol. 7, No. 5, pp. 573-585, DOI: 10.5897/SRE11.1724.

Sekulić, D., Dedović, V., Rusov, S., Šalinić, S., and Obradović, A. (2013). "Analysis of vibration effects on the comfort of intercity bus users by oscillatory model with ten degrees of freedom*." Applied Mathematical Modelling*, Vol. 37, No. 18, pp. 8629-8644, DOI: 10.1016/j.apm.2013.03.060.

Shi, X., Cai, C., and Chen, S. (2008). "Vehicle induced dynamic behavior of short-span slab bridges considering effect of approach slab condition." *Journal of Bridge Engineering*, Vol. 13, No. 1, pp. 83-92, DOI: 10.1061/(ASCE)1084-0702(2008)13:1(83).

Shi, X. and Cai, C. (2009). "Simulation of dynamic effects of vehicles on pavement using a 3D interaction model." *Journal of Transportation Engineering*, Vol. 135, No. 10, pp. 736-744, DOI: 10.1061/(ASCE) TE.1943-5436.0000045.

Snæbjörnsson, J. T., Baker, C., and Sigbjörnsson, R. (2007). "Probabilistic assessment of road vehicle safety in windy environments." *Journal of Wind Engineering and Industrial Aerodynamics,* Vol. 95, No. 9, pp. 1445-1462, DOI: 10.1016/j.jweia.2007.02.020.

Stark, T. D., Olson, S. M., and Long, J. H. (1995). *Differential movement at*

the embankment/structure interface-mitigation and rehabilitation, Rep. No. IAB-H1, FY 93, Illinois DOT, Springfield, Ill.

Wahls, H. E. (1990). *Design and construction of bridge approaches*, NCHRP Rep. No. 159, Transportation Research Board, National Research Council, Washington, D.C.

Wang, T. L. and Huang, D. (1992). "Cable-stayed bridge vibration due to road surface roughness." *Journal of Structural Engineering*, Vol. 118, No. 5, pp. 1354-1374, DOI: 10.1061/(ASCE)0733-9445(1992)118:5(1354).

White, D. J., Mekkawy, M. M., Sritharan, S., and Suleiman, M. T. (2007). "Underlying" causes for settlement of bridge approach pavement systems." *Journal of Performance of Constructed Facilities*, Vol. 21, No. 4, pp. 273-282, DOI: 10.1061/(ASCE)0887-3828(2007)21:4(273).

Yin, X., Cai, C., Fang, Z., and Deng, L. (2010). "Bridge vibration under vehicular loads: Tire patch contact versus point contact." International Journal of Structural Stability and Dynamics, Vol. 10, No. 3, pp. 529-554, DOI: 10.1142/S0219455410003609.

Yu, Y., Deng, L., Wang, W., and Cai, C. S. (2015). "Local impact analysis for deck slabs of prestressed concrete box-girder bridges subject to vehicle loading." *Journal of Vibration and Control*, DOI: 10.1177/1077546315575434.

Zhang, H. L. and Hu, C. S. (2007). "Determination of allowable differential settlement in bridge approach due to vehicle vibrations." *Journal of Bridge Engineering*, Vol. 12, No. 2, pp. 154-163, DOI: 10.1061/(ASCE)1084-0702(2007)12:2(154).

Zhang, W. and Cai, C. (2011). "Fatigue reliability assessment for existing bridges considering vehicle speed and road surface conditions." *Journal of Bridge Engineering*, Vol. 17, No. 3, pp. 443-453, DOI: 10.1061/(ASCE)BE.1943-5592.0000272.